Calculation of the Coulomb broadening of donor-acceptor pair emission in compensated semiconductors

P. Bäume, M. Behringer, J. Gutowski, and D. Hommel
Institut für Festkörperphysik, Universität Bremen, P.O. Box 330440, D-28334 Bremen, Germany
(Received 7 January 1999; revised manuscript received 3 February 2000)

The line shape of donor-acceptor pair luminescence bands in doped but partially compensated semiconductors exhibits a distinct broadening effect with increasing compensation ratio. We present a very sensitive Monte Carlo simulation of pair band emission highly suitable for typical compensated materials such as ZnSe:N, serving not only as a model material but being also of high-technological relevance. For low compensation, the line shape of the pair bands is calculated by taking into account the shift of the recombination energies due to charged impurities resulting in a very good agreement with the experiment. The model is perfectly applicable also to codoped ZnSe:N:Cl with Cl allowing for a precise control of the compensation ratio. By modelling the line shapes and comparing with the experiment, the density of compensating impurities could be determined even to values as low as several 10^{16} cm^{-3}. However, for high-compensation ratios, the model fails because relaxation between the excited donor-acceptor pairs is neglected.

I. INTRODUCTION

Donor-acceptor pair (DAP) bands have been widely used for more than three decades in order to characterize doped and partially compensated semiconductors. Extensive theoretical work has been done in the pioneering papers of Thomas, Hopfield, Augustyniak, and later Colbow.[1–3] The broad pair bands were explained in terms of radiative recombination of electrons trapped on donors with holes trapped on acceptors. The dominant broadening mechanism of the bands is the Coulomb interaction of nearest-neighbor donor-acceptor pairs. Further broadening mechanisms are related to phonon interaction. This theoretical approach is known as the DAP standard theory. However, even in the most profound work of Thomas *et al.*[2] some arbitrary broadening effect on the DAP line shape is included in the line shape calculations. The physical reasons for that additional broadening effect are manifold. The authors of Ref. 2 mentioned, e.g., phonon interaction and the Coulomb interaction of charged impurities surrounding the radiating DA pairs.

The broadening effect due to charged impurities was calculated by Breitenstein and Unger assuming a Gaussian line shape of each individual pair line.[4] Their work was thus capable of explaining why discrete pair spectra are hardly observable in compensated semiconductors. More recently, the benefits and limits of the DAP standard theory have been investigated in the field of the Group-II–VI semiconductors,[5] which are of technological interest since more than a decade. For weakly compensated samples, the DAP standard theory holds and allows for the determination of, e.g., binding energies and recombination rates of the impurities involved. For more strongly compensated samples, this theory is not capable of describing the considerably broadened and redshifted luminescence bands.[6–8] In Refs. 6–8, a qualitative explanation of the experimental observations is given taking into account the influence of charged impurities on the recombination energies. A first approach in terms of a Monte Carlo calculation of the DAP line shape in strongly compensated ZnSe was given in our previous work.[9] However, relaxation of the photogenerated carriers had to be assumed therein in order to explain the magnitude of the redshift of the experimental DAP line shape. Recently, an analytical approach for heavily doped and compensated ZnSe:N was presented by Kuskovsky *et al.*[10]

The purpose of the present paper is to develop a simple and reliable Monte Carlo calculation of the DAP line shape in moderately doped and weakly compensated semiconductors at low-excitation densities. For the very first time, a DAP line shape calculation, purely based on physical mechanisms, well-established to occur in the relevant materials, perfectly reproduces the experimental findings. No arbitrary broadening needs to be included in the calculations.

The paper is organized as follows: After a short description of the experimental technique (Sec. II), the standard DAP approach is briefly reviewed in the theoretical Sec. III. The influence of charged impurities is then included following the work of Shklovskii and Efros.[11] Subsequently, the Monte Carlo approach is presented. The standard line shape analysis of ZnSe:N (Sec. IV A) is then compared to the more powerful Monte Carlo approach (Sec. IV B). The Monte Carlo approach is further verified by the investigation of intentionally codoped ZnSe:N:Cl. Finally, the Monte Carlo approach is shown to fail for high-compensation ratios due to the relaxation of carriers in the warped band structure in the presence of potential fluctuations.

II. EXPERIMENTAL DETAILS

The ZnSe:N and ZnSe:N:Cl samples were grown in a twin chamber molecular-beam epitaxy system EPI 930. Nitrogen doping was performed using a rf plasma source. While sample A was exclusively nitrogen doped, samples B–D were codoped using the rf source and, additionally, a $ZnCl_2$ cell. The amount of incorporated chlorine donors was controlled by the temperature of the ZnSe:Cl effusion cell (see Table I). Details of the sample preparation prior to growth are published elsewhere.[12] The carrier concentration

TABLE I. Sample parameters. Samples B,C, and D were grown under identical conditions except for the temperature of the $ZnCl_2$ effusion cell.

Sample	Doping	$(N_A-N_D)[\mathrm{cm}^{-3}]$	$N_{\mathrm{Cl}}[\mathrm{cm}^{-3}]$	Excitation conditions
A	N	1.8×10^{17}		2 W/cm^2 at 430 nm (Figs. 1) 5 mW/cm^2 at 441.6 nm (Figs. 3 and 4)
B	N,Cl	not measurable	0.3×10^{17}	1 mW/cm^2 at 441.6 nm
C	N,Cl	4.7×10^{17}	1.2×10^{17}	1 mW/cm^2 at 441.6 nm
D	N,Cl	not measurable	2.3×10^{17}	1 mW/cm^2 at 441.6 nm

of sample C was characterized by an electrochemical capacitance-voltage (ECV) profiler. The donor and acceptor concentrations of sample B and D had to be estimated from the ECV measurement of sample C together with a calibration of the chlorine doping using a ZnSe:Cl multilayer with different $ZnCl_2$ temperatures during growth. The photoluminescence spectra were recorded at 1.6 K with above-band-gap excitation at 430 nm from a cw dye system or near-band-gap excitation at 441.56 nm from a HeCd laser. The excitation power ranges from several mW/cm^2 to 2 W/cm^2.

III. THEORY

A. Line shape according to the standard DAP model

For lightly p-doped and weakly compensated semiconductors with acceptor and donor concentrations N_A and N_D, respectively, the DAP standard theory was developed by Thomas *et al.*,[2] Colbow,[3] and was later applied by Bäume *et al.*[5] In the latter work, the intensity of transitions from neutral donors to neutral acceptors separated by a pair distance r is given as

$$I_k(r)dr \sim N_A g(r)dr f_e(r) W(r) \sigma_k . \tag{1}$$

Here, $I_k(r)$ represents the line shape of the DAP emission under the simultaneous creation of k LO phonons. $g(r)dr$ is the pair distribution function, $f_e(r)$ the steady-state fraction of neutral DA pairs, $W(r)$ the recombination rate, and σ_k the probability for the creation of k LO phonons with energy E_{LO}. The relation between pair separation r and the energy E of an emitted photon reads

$$E = E_{gap} - E_D - E_A + E_C - k\times E_{LO}; \quad E_C = \frac{e^2}{4\pi\epsilon_o\epsilon(0)r}. \tag{2}$$

The relation between Coulomb term E_C and pair separation r can be used to express the emitted intensity I as a function of the photon energy E

$$I(E) \sim \sum_{k=0}^{\infty} I_k[E-(E_{gap}-E_D-E_A)+k\times E_{LO}] \times \Theta[E-(E_{gap}-E_D-E_A)+k\times E_{LO}]. \tag{3}$$

The heavyside function Θ cancels out contributions with a negative Coulomb term. Equation (3) can be directly used to calculate the line shape of the DAP emission for the purpose of comparison with the experiment. However, the calculation is restricted to isolated, noninteracting DA pairs.

Depending on the experimental conditions, improvements of Eq. (3) can be made: For high densities of neutral impurities, which is the case for high doping and low compensation, each pair is surrounded by a background of neutral impurities of the majority dopant. The same is valid in more strongly compensated samples at high-excitation densities, where the major part of the charged impurities becomes neutralized via light-induced carriers. The background of neutral impurities generates additional recombination channels as being reported by Thomas *et al.*[2] These additional recombination channels sensitively influence the decay characteristics of the time-resolved luminescence of the pair bands.[13] The validity of Eq. (3) is therefore restricted to the luminescence bands of lightly doped and low-compensated samples.

B. Influence of charged impurities

It is well known that even in ZnSe made sucessfully p type, e.g., by the meanwhile established nitrogen doping methods, a considerable number of donors is builtin, leading to a particular compensation. Assume N_A the concentration of doped-in acceptors and $N_D < N_A$ that of compensating donors. Without light illumination, all donor electrons will have recombined into acceptors so that all donors are charged, $N_D^+ = N_D$. Likewise, $N_A^- = N_D$ acceptors are charged while $N_A - N_D$ acceptors remain neutral. For the concentration of charged impurities being sufficiently large, i.e., the compensation ratio being sufficiently high, each DA pair will be surrounded by a background of charged impurities and Eq. (2) is no longer valid for the photon energy of the DAP recombination. We modelled the charged surroundings of DA pairs by a Monte Carlo simulation method: Following Shklovskii and Efros,[11] we calculated the lowest total-energy state called pseudo-ground-state of a compensated p-type crystal with donor and acceptor concentrations N_D, N_A. The total energy H is minimized with respect to all possible transfers of a hole from a neutral acceptor to a charged one.

$$H=\frac{e^2}{4\pi\epsilon_o\epsilon(0)}\left[\frac{1}{2}\sum_{k}^{Acc}\sum_{k'\neq k}^{Acc}\frac{(1-n_k)(1-n_{k'})}{|r_k-r_{k'}|}-\sum_{k}^{Acc}\sum_{i}^{Don}\frac{1-n_k}{|r_i-r_k|}+\frac{1}{2}\sum_{i}^{Don}\sum_{j\neq i}^{Don}\frac{1}{|r_i-r_j|}\right] \quad (4)$$

n_K is an occupation number of acceptor k, where $n_k=1(n_k=0)$ indicates the acceptor to be neutral (charged). The first (third) term describes the repulsive interaction between two acceptors (donors), if and only if both are charged. The second term gives the attractive interaction between charged acceptors and donors. In a partially compensated semiconductor described by Eq. (4), each electron located at an impurity site i now exhibits an energy deviation ε_i from the binding energy of an electron located at an isolated impurity. This deviation is caused by the Coulomb potential of all other charged impurities and can be expressed as

$$\varepsilon_i=\frac{e^2}{4\pi\epsilon_o\epsilon(0)}\left[-\sum_{l\neq i}^{Don}\frac{1}{|r_i-r_l|}+\sum_{k\neq i}^{Acc}\frac{1-n_k}{|r_i-r_k|}\right]. \quad (5)$$

For lowest excitation densities in a photoluminescence experiment, the one-particle energies ε_i remain nearly unchanged compared to the light-off situation as the number of charged impurities stays nearly constant.

Consider a donor acceptor pair with pair distance r_{ij} and an initial state D^+A^-. By photoabsorption, the electron at the acceptor moves to the donor so that a D^oA^o state is created. The photon energy being emitted due to the electron transfer from donor i to acceptor j taking into account all Coulomb potentials can be calculated, if Shklovskii's and Efros'[11] expression for the change $\Delta_{i\rightarrow j}$ of the total energy H caused by the transition of one electron from donor site i to donor site j separated by a distance r_{ij}, is utilized,

$$\Delta_{i\rightarrow j}=\varepsilon_j^{Don}-\varepsilon_i^{Don}-\frac{e^2}{4\pi\epsilon_o\epsilon(0)r_{ij}}, \quad (6)$$

where ε_j^{Don} and ε_i^{Don} have to be calculated in the unperturbed system before the transition of the electron. Equation (6) remains valid for transitions of an electron between an acceptor and a donor, as far as the energy gap between donor and acceptor level is taken into account. First, we calculated the energy change ΔE of H due to a transition of an electron from acceptor site j to donor site i. The change of H can be calculated for this process $A_j^-D_i^+\rightarrow A_j^0D_i^0$ according to Eq. (6)

$$\Delta E=\Delta_{j\rightarrow i}=\varepsilon_i^{Don}-\varepsilon_j^{Akz}-\frac{e^2}{4\pi\epsilon_o\epsilon(0)r_{ij}}. \quad (7)$$

For convenience, the principal energy difference $(E_{gap}-E_D-E_A)$ between the undisturbed impurity levels of donor and acceptor has been omitted in Eq. (7). Naturally, the reverse process $D_i^0A_j^0\rightarrow D_i^+A_j^-$ causes a change of H by $-\Delta E$. If this change in energy $-\Delta E<0$, the system becomes more tightly bound and the photon energy $\hbar\omega$ of the DAP recombination process is increased by $+\Delta E$, thus amounting to

$$\hbar\omega=E_{gap}-E_D-E_A+\varepsilon_i^{Don}-\varepsilon_j^{Acc}-\frac{e^2}{4\pi\epsilon_o\epsilon(0)r_{ij}}. \quad (8)$$

It should be mentioned that ΔE contains the nearest-neighbor Coulomb term of the donor-acceptor pair as well as the electrostatic contributions of all other charged impurities in the crystal. Consequently, Eq. (8) is reduced to Eq. (2) if the crystal would contain only one donor D_i^+ and one acceptor A_j^-. The same approach works when calculating the recombination energy for an D^0A^0 pair, which was initially a D^+A^0 pair:

$$\hbar\omega=E_{gap}-E_D-E_A+\varepsilon_i^{Don}-\varepsilon_j^{Acc}. \quad (9)$$

The lack of the nearest-neighbor Coulomb term in Eq. (9) is, at a first glance, somewhat surprising. However, this term is hidden in the one-particle energies ε_i as they have to be calculated in the undisturbed system in the absence of light.

The Monte Carlo simulation, using the formulas derived so far, consists of the following: A simulated zinc-blende lattice L^3 is randomly populated with N_DL^3 donors and N_AL^3 acceptors. As mentioned above, for p-type crystals, all donors are initially positively charged. $(N_A-N_D)L^3$ acceptors are neutral, the remaining N_DL^3 acceptors are negatively charged. The positions of the charges are initially arbitrary. A subsequent minimization of the total energy H yields a pseudoground state where all the one-particle states [Eq. (5)] are known. Each individual nearest-neighbor pair i in the simulated crystal with pair separation r_i and recombination energy E_i [Eqs. (5), (8), and (9)] radiates with an intensity $I_i(r_i)$

$$I_i(r_i)=f_e(r_i)W(r_i), \quad (10)$$

where $f_e(r_i)$ is the steady-state fraction of neutral pairs with pair separation r_i. The line shape $I_{sum}(E)$ of the zero-phonon band of the DAP then consists of a superposition of all radiating nearest-neighbor pairs

$$I_{sum}(E)dE=\sum_i I_i(r_i) \quad (11)$$

with i running over all pairs with recombination energy in $[E,E+dE]$.

Finally, the intensities of the LO-phonon replicas k have to be calculated with phonon coupling constants proportional to σ_k taken directly from the experiment

$$I_k(E)=I_{sum}(E)\sigma_k. \quad (12)$$

The superposition of the replicas including the zero-phonon band yields

$$I(E)\sim\sum_{k=0}^{\infty}I_k(E+k\times E_{LO}), \quad (13)$$

where terms with $k>4$ turn out to be negligible when compared to the experiment. Equation (13) can then be directly compared to the experimental DAP line shapes of weakly compensated and weakly excited semiconductors.

Summarizing, the deviation of the analytical calculation following Eq. (3) from the Monte Carlo simulation presented here, consists of two points: First, the continuous pair distri-

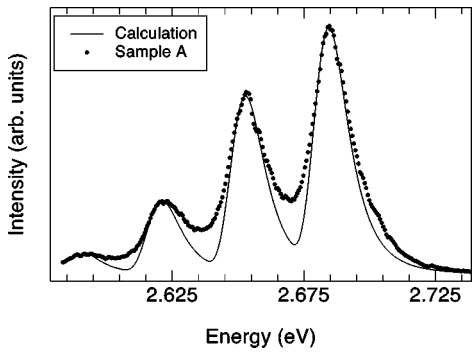

FIG. 1. Calculated photoluminescence of a lightly doped and weakly compensated ZnSe:N sample with $[N_A-N_D]=1.8\times10^{17}$ cm^{-3} in the framework of the DAP standard theory [Eq. (3)]. The experimental spectrum at 1.6 K was obtained under excitation with 2W/cm^2 at 430 nm.

bution $g(r)dr$ is replaced by a simulated zinc-blende lattice L^3. Second, the recombination energy of each DAP process is calculated via Eqs. (5), (8), and (9) and not via Eq. (2). All other features of the standard theory remain unchanged.

IV. RESULTS AND DISCUSSIONS

A. Standard line shape analysis

In order to show the benefits and limits of the standard line shape analysis, we calculated theoretical line shapes following Eq. (3). The results were compared to the donor-acceptor-pair bands of the lightly doped and low-compensated ZnSe:N sample A with $[N_A-N_D]=1.8\times10^{17}$ cm^{-3}. A fit to an experimental spectrum obtained for an excitation density of 2W/cm^2 is depicted in Fig. 1. The sample parameters and the parameters of the calculation are displayed in Tables I and II, respectively. The experimental line shape refers exclusively to electronic transitions from deep, nitrogen-related donors to shallow nitrogen acceptors, as has been confirmed by excitation-density dependent spectroscopy and selective pair luminescence (not shown). The excitation density was large enough as to minimize the number of charged impurities that makes the standard line shape analysis applicable. For even higher-excitation densities, a competing DAP series appears as high-energy shoulders of the principal DAP series (not depicted). This result indicates that an effective transfer of electrons takes place from shallow donors to deep, nitrogen-related donors, however, the latter being saturated at higher-excitation densities. Beyond the saturation density, electron transitions from shallow donors to shallow acceptors generate the second DAP series. The result of the theoretical calculation best matching the experimental line shape is depicted as a solid line in Fig. 1. The agreement with the experiment is quite good on the high-energy side of the DAP bands. However, the broadening or smearing of the minima between the zero-phonon band and between the phonon replicas as apparent in the experimental spectra is not reproduced by the standard approach [Eq. (3)].

The model parameters (Table II) used for the calculation are in excellent agreement with those derived in our previous work on time-resolved luminescence of ZnSe:N, where the full Thomas-Hopfield approach, including the ensemble average over different donor surroundings, was applied.[13] We found $E_D=51.5$ meV for the deep donor and an effective Bohr radius of 2.25 nm calculated utilizing the so-called scaled effective-mass theory.[14] This is essentially the same approach as mentioned by Ridley[15] when treating core effects. It reads

$$a_{D/A}=\sqrt{\frac{E^*_{D/A}}{E_{D/A}}}\times a^*_{D/A}, \tag{14}$$

where $E^*_{D/A}$, $a^*_{D/A}$ are the energies and Bohr radii of the donor and the acceptor obtained in the effective-mass approximation, respectively (see Table II). For the shallow nitrogen acceptor we used the well-established ionization energy of $E_A=110$ meV (Ref. 16) yielding an effective Bohr radius of 0.54 nm. The best fit is obtained if the concentration of the major impurity species is set to $[N_A]=2.3\times10^{17}$ cm^{-3} resulting in $[N_D]=0.5\times10^{17}$ cm^{-3} since $[N_A-N_D]$ is fixed to 1.8×10^{17} cm^{-3} as obtained by CV profiling. The line shape is further determined by the steady-state occupation number $f_e(r)$ of excited pairs, where the

TABLE II. Parameters of the calculation in the standard model and of the Monte Carlo calculations. Binding energies $E_D^N=51.5$ meV, $E_A^N=110$ meV. Effective Bohr radii $a_D^N=2.25$ nm, $a_A^N=0.54$ nm are calculated as $a^N_{D/A}=\sqrt{E^*_{D/A}/E^N_{D/A}}\times a^*_{D/A}$ using effective mass values $a_A^*=0.46$ nm, $a_D^*=3.22$ nm, $E_D^*=25.2$ meV, and $E_A^*=151$ meV. Recombination rate (deep N-donor to shallow N-acceptor) $W_0=3\times10^8$ s^{-1}. Static dieelectric constant $\epsilon(0)=8.88$. Phonon-coupling parameters σ_k: Sample A, Fig. 1: $\sigma_0=1$, $\sigma_1=0.73$, $\sigma_2=0.30$, $\sigma_3=0.1$. Sample A, Fig. 3: $\sigma_0=1$, $\sigma_1=0.68$, $\sigma_2=0.25$, $\sigma_3=0.07$. Samples B,C, and D: $\sigma_0=1$, $\sigma_1=0.72$, $\sigma_2=0.28$, $\sigma_3=0.08$.

Sample	N_A[cm^{-3}]	N_D[cm^{-3}]	$\gamma\alpha$[m^{-2}s^{-1}]	Calculation type
A, Fig. 1	2.3×10^{17}		5.3×10^{22}	Standard
A, curve ''0.5'' Fig. 3	2.3×10^{17}	0.5×10^{17}	5×10^{20}	Monte Carlo
B, Fig. 4	6.9×10^{17}	1.3×10^{17}	5×10^{21}	Monte Carlo
C, Fig. 4	6.9×10^{17}	2.2×10^{17}	5×10^{20}	Monte Carlo
D, Fig. 4	6.9×10^{17}	3.3×10^{17}	5×10^{20}	Monte Carlo

only free parameter is the ratio $W_o/(\gamma\alpha)$ with recombination constant W_o, generation rate of photocarriers γ and α being the prefactor of the capture cross section $\sigma(r)=\alpha\times r^2$ for photoneutralization as derived by Thomas *et al.*[2]

The theoretical line shape is sensitive to the binding energies of donor and acceptor as they determine the magnitude of the Coulomb term. Further, it is sensitive to the wave function size of the more loosely bound particle and to $W_o/(\gamma\alpha)$. It is much less sensitive to moderate changes of the major impurity concentration. The line shape is quite robust against changes of the wave function size of the more tightly bound hole at the acceptor. Thus, a determination of the acceptor binding energy in ZnSe:N can be performed even if details of the wave function of the acceptor are omitted.

In conclusion, we showed that the standard approach after Eq. (3) works well, if the doping concentration and the concentration of charged impurities due to compensation are low enough. The latter can be achieved by using sufficiently high excitation densities further minimizing the charge densities by photoneutralization. We further showed agreement to our previous work on the time-resolved luminescence of donor-acceptor pair bands: Both the time-resolved and the time-integrated luminescence can be described using the same set of parameters for the impurity binding energies and Bohr radii. However, when looking into the details (low-energy tails of the bands in the regime between the LO bands) the standard procedure turned out to be of still not satisfying quality at any excitation density.

B. Monte Carlo simulations

In this section, the luminescence line shapes of donor-acceptor bands in the limit of lowest excitation densities are investigated. The influences of the charged impurities in partially compensated samples not being photoneutralized should broaden the line shape. These broadening effects will be calculated and the concentration of the charged impurities will be estimated.

Once the details of the impurities involved such as binding energies and effective Bohr radii are known, there are, in principle, three independent parameters left that may be changed in a Monte Carlo approach to calculate the variety of different line shapes that are experimentally observed. Two of these are the donor and acceptor concentrations, however, being interdependent if the carrier concentration is known from, e.g., ECV profiling. Furthermore, the excitation level expressed by $W_o/(\gamma\alpha)$ can be varied. However, also W_0 was not freely set in the present calculations but has been independently determined for our ZnSe:N samples through the analysis of time-resolved DAP decay, which we already performed in Ref. 13. Thus, for known N_A-N_D and predetermined W_0, the fit is restricted to a variation of the parameter N_D. This restriction makes the model quite valuable if the experimental results are nicely met, as will be shown below.

Figure 2 displays the influence of the internal electric fields on the recombination energies of nearest-neighbor donor-acceptor pairs in a simulated zinc-blende lattice with $[N_A]=2.3\times10^{17}$ cm^{-3} and $[N_D]=0.5\times10^{17}$ cm^{-3} and containing 100 donors. A minimization of the total energy H of the system [Eq. (4)] has been carried out with respect to one-particle transitions, and the one-particle energies ε_i [Eq. (5)] were calculated. Each point in Fig. 2 represents one pair of separation r with a Coulomb term of the radiative recombination calculated with Eqs. (8) and (9) (for convenience, the energy gap between donor and acceptor level is set to zero). The calculated points scatter around a curve displaying the standard-theory Coulomb term $e^2/(4\pi\epsilon_o\epsilon(0)r)$. For this curve, the electrostatic potential of all charged impurities, except that of the nearest neighbor is omitted.

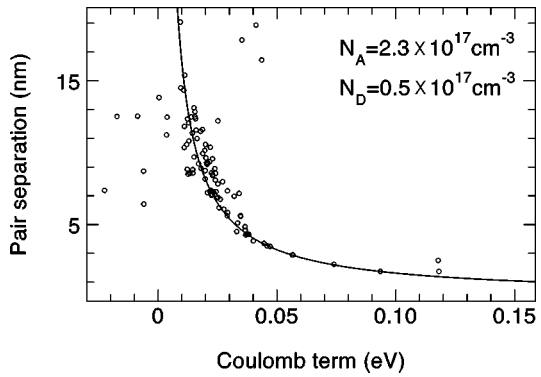

FIG. 2. Calculated Coulomb energy (dots) of the DAP recombination in p ZnSe [$\epsilon(0)=8.88$] with $N_A=2.3\times10^{17}$ cm^{-3} and a compensation ratio $K=N_D/N_A=0.33$. The curve represents the Coulomb energy in the standard model for the limiting case $K\rightarrow0$.

The data thus gained can be used to calculate the DAP line shape via Eq. (13). Each nearest-neighbor pair with pair separation r_i and recombination energy E_i [Eqs. (8) and (9)] radiates with an intensity $f_e(r_i)W(r_i)$ [Eq. (10)]. These individual emission lines are superimposed and the phonon replicas are calculated [Eq. (12)]. To improve the signal-to-noise ratio of the Monte Carlo simulation, the procedure was repeated with several hundred different simulated lattices L^3, and the average of the simulated luminescence bands was taken.

The results of the Monte Carlo simulation applied to sample A are displayed in Fig. 3. The experimental line shape of the DAP band has been obtained at a very low-excitation density of 5 mW/cm^2 thus minimizing the effects of neutralization of charged impurities and of screening of the charges via photocarriers, and is given as dotted curves repeated behind each fit curve to allow for easy comparison. For the fits, the same parameters were used as for the standard analysis, except for the donor and acceptor concentrations N_D and N_A. $[N_A-N_D]=1.8\times10^{17}$ cm^{-3} as derived from ECV profiling and the model excitation density expressed by $\gamma\alpha$ were kept constant (see Table II). For a very low-donor concentration of $[N_D]=0.1\times10^{17}$ cm^{-3}, the Monte Carlo simulation reproduces the standard line shape (not shown in Fig. 3), provided the same parameters are used for both calculations. With increasing donor concentration and all other parameters held constant, the line shape obtained in the simulation broadens and the band peaks shift slightly to higher energies. For $[N_D]=0.5\times10^{17}$ cm^{-3}, a perfect agreement between the experimental line shape and the simulation is achieved. For further increasing donor concentration, the simulated line shape becomes broader than the experimental line shape. The whole development clearly

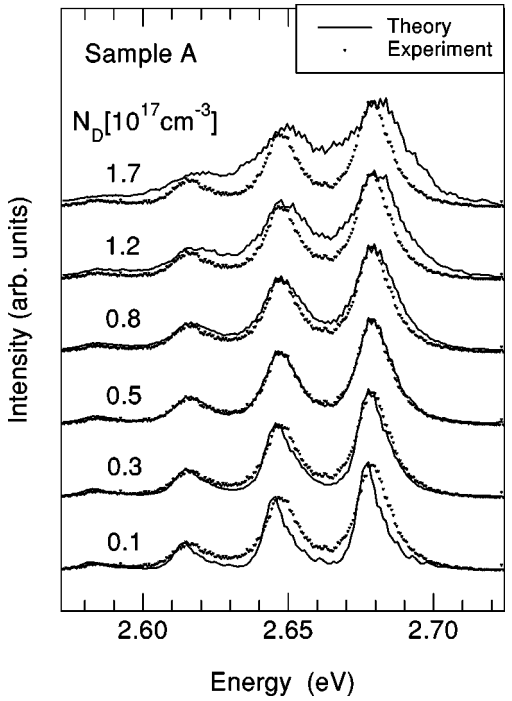

FIG. 3. Comparison of different Monte Carlo simulations (solid curves) with one experimental spectrum of a lightly doped sample (dotted line) excited with 5 mW/cm^2 at $\lambda = 441.56$ nm. For the simulations, the experimentally determined value of $[N_A - N_D] = 1.8 \times 10^{17}$ cm^{-3} is kept fixed while the donor concentration N_D is varied as labeled in the figure in units of 10^{17} cm^{-3}. All other parameters of the simulations are identical.

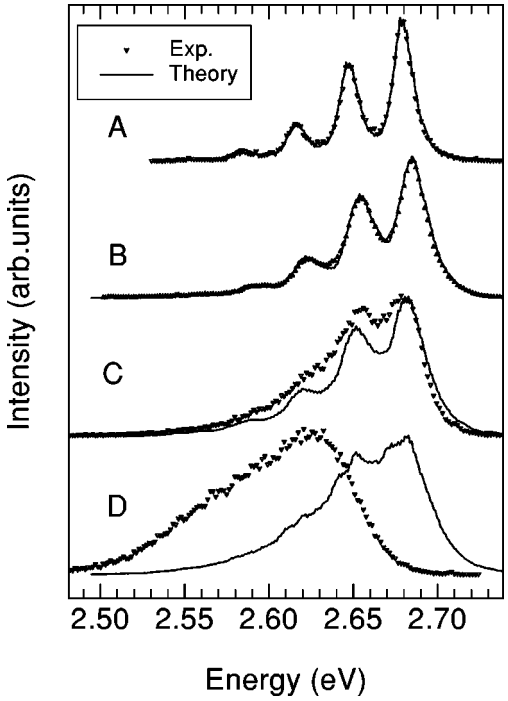

FIG. 4. Comparison of the photoluminescence (dotted curves) of different ZnSe:N—and codoped ZnSe:N:Cl—samples to theoretical line shapes derived from Monte Carlo simulations (solid curves). The details of doping and of the electrical properties of the samples A to D are displayed in Table I.

indicates the sensitivity of the model calculations to changes in the number of donors and thus to the number of charged impurities.

We would like to emphasize, that this line shape calculation of donor-acceptor pair bands is fully describing the experimental spectra. Moreover, our Monte Carlo approach contains no arbitrary broadening mechanism. The results of the calculations show that even very low compensation with several 10^{16} cm^{-3} donors is capable of producing a distinct broadening effect. A further benefit of this approach is the precise determination of the concentration of the compensating donors, if additional information concerning the free-carrier concentration $[N_A - N_D]$ is available from, e.g., ECV profiling.

We further simulated the photoluminescence of codoped ZnSe:N:Cl samples (sample B, C, D, see Tables I and II and Fig. 4) that provide a precise control over the amount of incorporated shallow chlorine donors.[17] However, the samples contain an unknown quantity of deep and shallow nitrogen-related donors unintentionally builtin during the intended *N* acceptor doping procedure. The experimental results for the photoluminescence spectra at 2 K and low-excitation density are compared to the calculations in Fig. 4, labeled B–D according to the sample notations. For comparison, the luminescence and the best matching Monte Carlo simulation of sample A are displayed in Fig. 4 and labeled A, too. Although the samples B–D contain a considerable amount
of shallow chlorine donors with a binding energy of $26 \ldots 28$ meV,[16] there is no experimental evidence for a second DAP series involving transitions from shallow chlorine donors to shallow nitrogen acceptors. We concluded on efficient relaxation channels between shallow and deep donors and included exclusively the deep DAP series in our calculations. The shallow donors act only as charged D^+ centers that do not become photoneutralized.

The DAP series of sample B is shifted to higher energies and broadened compared to that of sample A. The doping level of sample B was higher than that of A, so we concluded that the amount of deep donors should likewise be enhanced. For trial concentrations of $[N_D] = 1.3 \times 10^{17}$ cm^{-3} being the sum of $[N_D^N] = 1.0 \times 10^{17}$ cm^{-3} and $[N_D^{Cl}] = 0.3 \times 10^{17}$ cm^{-3}, together with $[N_A] = 6.9 \times 10^{17}$ cm^{-3}, we achieved a very good correspondence between simulation and experiment.[18]

While all other growth parameters were kept constant, we increased the amount of incorporated chlorine to $[N_D^{Cl}] = 1.2 \times 10^{17}$ cm^{-3} (sample C). The DAP luminescence of sample C is strongly broadened and slightly redshifted compared to A and B being well explainable by the assumption of potential fluctuations. With all parameters except the model excitation density and the donor concentration being fixed to the values of simulation B, we again calculated the line shape based on the Monte Carlo simulations. However, the correspondence to the experiment is less satisfactory as the theoretical line shape is less broadened and redshifted than the experimental one. The same is found for sample D where $[N_D^{Cl}] = 2.3 \times 10^{17}$ cm^{-3} chlorine donors are incorporated. The experimental line shape is strongly broadened and shifted by more than 60 meV to lower energy with respect to the photoluminescence (PL) of fairly uncompensated

samples like sample A. For the model calculation D we used the same set of parameters as for simulation C except for the donor concentration that was set to $[N_D]=3.3\times10^{17}$ cm^{-3}. The strong deviations between model and experiment are obvious but not surprising. As has been pointed out by us already,[9] the luminescence of strongly compensated and highly doped semiconductors can only be successfully calculated if relaxation of the photogenerated carriers in the warped band structure in the presence of potential fluctuations is included. The applicability of the model developed in the present paper is therefore restricted to low degrees of compensation where relaxation between the excited pairs does not play an important role.

The mechanisms of the relaxation are only partially understood, because the approach of Bäume *et al.*[9] is restricted to relaxation between excited pairs thus neglecting other mechanisms as the intraband relaxation between photogenerated carriers. This leads to an imperfect agreement between the simulation and the experimental data. However, at low compensation the approach presented here is more precise and reliable than any earlier treatment. Furthermore, the determination of the concentration of the minor impurity species is of special interest in the case of low compensation, which can now be rather exactly determined at uniquely low limits.

V. CONCLUSIONS

We presented the first calculations of the line shape of donor-acceptor pairs in partially compensated semiconductors fully including the influence of charged impurities on the recombination energies. The simulations neglect other broadening effects such as the strain broadening or inhomogeneous doping level and defect concentration. However, we proved that the Coulomb broadening including the electrostatic interaction of the charged-impurity environment of the DA pairs is by far the dominant mechanism. The Monte Carlo approach was shown to work excellently for low-compensation ratios in p type ZnSe:N and codoped ZnSe:N:Cl. The amount of compensating donors could be precisely estimated with a limit as low as several 10^{16} cm^{-3} and with an accuracy of several 10^{16} cm^{-3}. For high compensation ratios, the model presented here fails since the relaxation of carriers in the warped band structure has been neglected.

[1] D. G. Thomas, J. J. Hopfield, and K. Colbow, *Physics of Semiconductors IV* (Academic Press, New York, 1964), p. 67.

[2] D.G. Thomas, J.J. Hopfield, and W.M. Augustyniak, Phys. Rev. **140**, A202 (1965).

[3] K. Colbow, Phys. Rev. **141**, 742 (1966).

[4] O. Breitenstein and K. Unger, Phys. Status Solidi B **91**, 557 (1979).

[5] P. Bäume, F. Kubacki, and J. Gutowski, J. Cryst. Growth **138**, 266 (1994).

[6] P.W. Yu and Y.S. Park, J. Appl. Phys. **50(2)**, 1097 (1978).

[7] H.P. Gislason, B.H. Yang, and M. Linnarsson, Phys. Rev. B **47(15)**, 9418 (1993).

[8] P. Bäume, J. Gutowski, D. Wiesmann, R. Heitz, A. Hoffmann, E. Kurtz, D. Hommel, and G. Landwehr, Appl. Phys. Lett. **69**, 1914 (1995).

[9] P. Bäume, J. Gutowski, and D. Hommel, *Proceedings of the 23rd Conference on the Physics of Semiconductors* (ICPS), edited by M. Scheffler and R. Zimmerman (World Scientific, Singapore, 1996).

[10] I. Kuskovsky, D. Li, G.F. Neumark, V.N. Bondarev, and P.V. Pikhitsa, Appl. Phys. Lett. **75**, 1243 (1999).

[11] B. I. Shklovskii and A. L. Efros, *Properties of Doped Semiconductors* (Springer-Verlag, Berlin, Germany, 1984).

[12] M. Behringer, P. Bäume, D. Hommel, and J. Gutowski, Phys. Rev. B **57**, 12 869 (1998).

[13] P. Bäume, S. Strauf, J. Gutowski, M. Behringer, and D. Hommel, J. Cryst. Growth **184/185**, 531 (1998).

[14] G.J. Yi and G.F. Neumark, J. Lumin. **60/61**, 29 (1994).

[15] B. K. Ridley, *Quantum Processes in Semiconductors*, 3rd ed. (Oxford Science, Oxford, UK, 1993).

[16] J. Gutowski, N. Presser, and G. Kudlek, Phys. Status Solidi A **120**, 11 (1990); Landolt-Börnstein, *Semiconductors*, edited by O. Madelung, U. Rössler, and M. Schulz, Vol. III/41, Subvolume II-VI and I-VII Compounds, Semimagnetic Compounds (Springer-Verlag, Berlin, 1999), Chap. 3.7.

[17] Experimental results on codoping of ZnSe with N and Cl have been extensively discussed by us in Ref. 12, however, without any simulation treatment in the framework of the Monte Carlo approach.

[18] Unfortunately, electrical measurements of sample B and D, e.g., ECV profiling, failed for unknown reasons. The amount of incorporated chlorine was calculated from gauge measurements in pure ZnSe:Cl. The values N_A-N_D derived for these samples from the simulations reasonably agree with the trend (redshift and broadening) of the DAP bands for higher Cl concentrations.